

Synthesis of self-assembly of agarose-fatty acid ester nanoparticles

Stalin Kondaveeti^a, Dharmesh R Chejara^{a, b}, A K Siddhanta^{a, b, *}

^aMarine Biotechnology and Ecology Discipline, CSIR-Central Salt & Marine Chemicals Research Institute,
G B Marg, Bhavnagar 364 002, Gujarat, India

^bAcademy of Scientific & Innovative Research, Anusandhan Bhavan,
2 Rafi Marg, New Delhi 110 001, India

Email: aks@csmcri.org

Received 24 December 2013, revised and accepted 23 March 2014

Microwave assisted facile synthesis of hydrophobically modified nano-sized particulate esters of agarose and stearic and palmitic acids (Ag-SA and Ag-PA), employing carbodiimide chemistry has been described. The hydrophobically modified agarose is capable of forming self-assembled nano-sized particles. Physicochemical characterization of Ag-SA, Ag-PA has been carried out by gel permeation chromatography, differential scanning calorimetric, scanning electron microscopy and FT-IR, ¹³C-NMR and ¹H-NMR spectra. The aqueous self-assembly of the modified polymer has been studied by dynamic light scattering and transmission electron microscopy, which shows the formation of 4-5 nm micelles, and 220-250 nm polymeric vesicles. TEM images demonstrate that the self-aggregate is spherical in shape. These new agarose based nano-sized materials may be of potential utility in biomedical applications as drug delivery vehicles.

Keywords: Nanoparticles, Self-assembly, Hydrophobization, Natural polymers, Polysaccharides, Carbodiimides, Agarose, Fatty acid esters, Stearic acid, Palmitic acid, Microwave synthesis

Recently, there has been a growing interest in the hydrophobically modified derivatives of polysaccharides for biomedical applications. One of the main advantages of polysaccharides as natural biomaterials is their availability in natural resources and low-cost processing, which make them very accessible materials to be used in pharmaceutical applications. Furthermore, polysaccharides possess several favorable characteristics including biocompatibility, biodegradability, highly stable, safe, nontoxic and abundance of functional groups for modification or functionalization.^{1,2} The amphiphilic nature imparted upon polysaccharides after hydrophobic modification provides them with a wide and interesting domain of applications, viz., as rheology modifiers, emulsion stabilizers, surface modifiers for liposomes and nanoparticles, and as drug delivery vehicles.³⁻⁸

Hydrophobically modified polysaccharides such as starch, chitosan, dextran and pullulan can form self-assembled nanoparticles for biomedical uses.⁹ Some long-chain fatty acids like hexanoic acid, linoleic acid, linolenic acid, palmitic acid and stearic acid have been used for modifying polysaccharides and obtaining polymeric micelles. Nanoparticles based on linoleic acid-chitosan have been obtained through a carbodiimide-mediated reaction³, and their

size ranged between 200–600 nm. Stearic acid grafted chitosan oligosaccharide was synthesized by 1-ethyl-3-(3-dimethylaminopropyl) carbodiimide mediated coupling reaction.¹⁰ Aqueous self-assembled nano-sized polymeric micelles and vesicles of hydrophobically modified hydroxyethyl starch with the long chain fatty acids under mild reaction conditions using dicyclohexylcarbodiimide/4-dimethylaminopyridine (DCC/DMAP) have been reported.¹¹ The synthesis of modified hydrophobic starch using fatty acids was carried out with potassium persulphate as catalyst in DMSO and nanoparticles of starch were prepared by the dialysis method.¹² Dextran has also been employed to obtain nanoparticles by coupling lipoic acid to the structure of dextran and forming nanoparticles (145–221 nm) in water.¹³ After the modification step, the self-assembled nanoparticles, based on hydrophobically modified polysaccharides, were prepared by various methods.¹⁴⁻¹⁹

Wang *et al.*²⁰ reported the preparation and characterization of protein-containing agarose hydrogel nanoparticles prepared by using emulsion-converted-to-suspension *in situ* method. Preparation of agarose based metal/semiconductor nanoparticles composite films by introducing the metal/semiconductor precursor

solution followed by a reducing agent during the gelation process of agarose has been reported.²¹ Agarose-stabilized gold nanoparticles for surface-enhanced Raman spectroscopic detection of DNA nucleosides were reported by Kattumuri *et al.*²² and Zhang *et al.*²³ reported characterization of the aminated agarose labeled with fluorescein isothiocyanate resulting in fluorescent nanoparticles.

Agarose, the red seaweed polysaccharide is widely used in biomedical and bioengineering applications. The basic disaccharide repeating units of agarose consists of (1,3) linked β -D-galactose (G) and (1,4) linked α -L-3,6-anhydrogalactose (A).²⁴ Stearic and palmitic acids are widely used to produce soaps, cosmetics, and release agents. Microwave assisted esterification is one of the facile ways to modify polysaccharides. This technique has been used to prepare polysaccharide-based materials.²⁵⁻²⁸ Synthesis of polysaccharide ester conjugates using DCC and DMAP as activating agents for carboxylic acid have been studied.²⁹⁻³¹

Hydrophobically modified polysaccharides such as starch, chitosan, dextran and pullulan with long-chain fatty acids like hexanoic acid, linoleic acid, linolenic acid, palmitic acid and stearic acid have been described.⁹ However, to the best of our knowledge no reports on the hydrophobization of the natural polymer agarose with fatty acids are available in the literature. As part of a continuing program of modification of agarose with various substrates in our laboratory,^{27,28} we report herein the synthesis and characterization of hydrophobically modified self-assembled nano-sized new esters of agarose and saturated fatty acids.

Materials and Methods

Agarose was extracted from the red seaweed (*Gracilaria dura*) of Indian waters following the method reported in the literature.³² Stearic acid (SA), palmitic acid (PA), dicyclohexylcarbodiimide (DCC) and 4-dimethylaminopyridine (DMAP) were purchased from M/s. Spectrochem Chemicals Ltd., Mumbai, India. Milestone Start-S (Italy) programmable microwave reactor (model Start-S; Terminal T260; Line voltage 230 V; Magnetron S.N. 131528; Frequency 2450 Hz) was used for the reaction. The characterizations were done by FT-IR analysis using a Perkin-Elmer FT-IR spectrometer (Spectrum GX, USA) on a KBr disc (2 mg sample in 600 mg KBr). ¹³C-NMR spectra were recorded on a Bruker Avance-II 500 (Ultra Shield, Switzerland)

spectrometer, at 125 MHz. Samples (agarose, Ag-SA and Ag-PA) were dissolved in DMSO-*d*₆ (60 mg/mL) and spectra were recorded at ambient temperature (*ca.* δ 39.5 ppm).³³ The ¹³C NMR spectra of stearic acid and palmitic acid were recorded in CDCl₃ (30 mg/mL) at ambient temperature (*ca.* δ 77.0 ppm). The ¹H NMR spectra of agarose and derivatives (Ag-SA, Ag-PA) were recorded at ambient temperature (10 mg/mL of DMSO-*d*₆).

The molecular weights (M_n , M_w) and polydispersity index (PDI) were measured by gel permeation chromatography (GPC), performed on a Waters Chromatograph equipped with an ERC-7515A refractive index detector and Styragel columns (HR 0.5 DMF, HR 4E DMF and HR 5 DMF). The mobile phase was DMF, delivered at a flow rate of 0.8 mL/min using a Waters 515 isocratic pump. The MW calibration curve was based on eight polystyrene standards.

Differential scanning calorimetric (DSC) measurements were made on a Mettler Toledo DSC822 equipment (Switzerland), at a heating rate of 2 °C/min in the temperature range -20–25 °C, and at 10 °C/min in the temperature range 30–500 °C in separate experiments. The degree of substitution (DS) was determined by proton NMR (¹H-NMR). The peaks between 4.69 and 5.25 ppm corresponded to the signals from the four protons of the glycoside structure. The three protons of the CH₃ terminal of the acyl chain were observed at 0.84 ppm. The DS was obtained from the ratio of the area of the proton peak at 0.84 ppm to that of the proton peaks between 4.69 and 5.25.³⁴

Preparation and characterization of Ag-SA and Ag-PA

The self-aggregated nano-sized particles of Ag-SA and Ag-PA products were produced by a simple dialysis method. The modified polymer (Ag-SA/Ag-PA, 10 mg) was dissolved in 5 mL of dimethyl sulfoxide and stirred for 30 min. The solution was then added dropwise to 20 mL of water and stirred for another 3 h. The resultant solution was filtered through a 0.45 m syringe filter and used for different studies. This solution was poured into a dialysis bag (molecular weight cutoff 1200 Da), which was then immersed into 1 L of fresh water and stirred at room temperature. The DMSO was removed by dialysis with water in the beaker been replaced occasionally ($\times 3$ times) with water in a 24 h process. Then the solution inside the dialysis bag was filtered through a 0.45 m syringe filter and used for DLS, SEM and TEM studies.

The changes in morphology of the different samples (Ag-SA and Ag-PA) were determined using a scanning electron microscope (LEO 1430 VP, Carl-Zeiss, Germany), at an accelerating voltage of 20 kV. A small amount of the sample was mounted on the aluminum stub and placed in the vacuum chamber. All images were recorded at the same magnification.

TEM images were obtained using a transmission electron microscope (JEM 2100, JEOL) operated at an accelerated voltage of 200 kV. To measure the morphology and size distribution of the nano-sized particles, the samples were prepared by dropping the sample solution (0.1%) onto a carbon-coated copper grid. The copper grid was then dried at room temperature over 24 h and then vacuum dried and kept in a desiccator.

Self assembly of Ag-SA and Ag-PA

Dynamic light scattering (DLS) measurements were made at 298.15 K on a NaBiTec Spectro-Size 300 light scattering apparatus (NaBiTec, Germany) with a He-Ne laser (633 nm, 4 MW). A 0.5% solution each of Ag-SA or Ag-PA was filtered directly into the quartz cell using a membrane filter of 0.45 μm pore size. Prior to measurements, the quartz cell was rinsed several times with water (filtered through 0.45 μm membrane filter) and then filled with the filtered sample solutions. The temperature of the measurements was controlled with an accuracy of

0.1 K. The data evaluation of the dynamic light scattering measurements was performed with the inbuilt CONTIN algorithm.

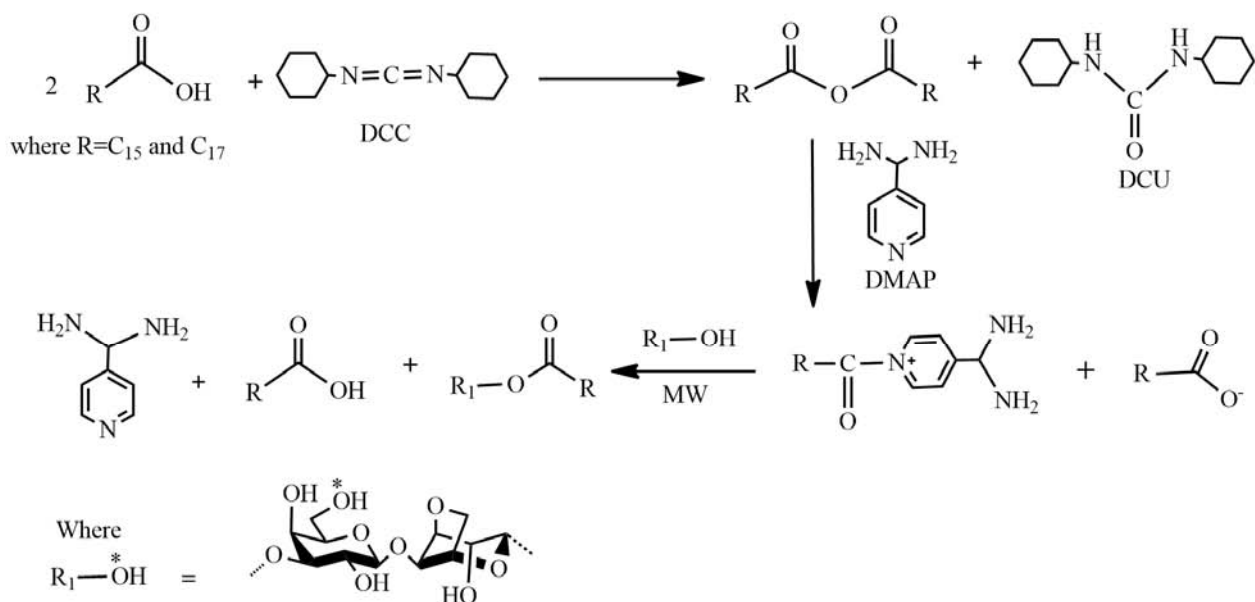
Results and Discussion

Synthesis of Ag-SA and Ag-PA

In a typical batch, the dried agarose (306 mg, 1 mmol) was dissolved in *N,N*-dimethylformamide (DMF) at 80 °C for 3 min in a microwave reactor under stirring. To the solution, were added a pre-solubilized mixture of fatty acids (stearic acid and palmitic acid 1 mmol), DCC (412 mg, 4 mmol) and DMAP (30.5 mg, 0.25 mmol) in DMF and the reaction was carried out under microwave irradiation (pulsed mode, 400 W) at 100 °C for 25 min. After completion of the reaction, the product was isolated by precipitation using *iso*-propyl alcohol (reaction mixture-IPA, 1:2 *v/v*). The precipitated product was washed with IPA (20 mL \times 4) under stirring (20 min for each wash) to remove excess of the reagents followed by drying under vacuum (Scheme 1).

Physicochemical properties

Optimization studies revealed that microwave irradiation for 25 min at 100 °C led to the formation of the ester bond between the carboxy termini of fatty acids (stearic and palmitic acids) and hydroxyl groups of agarose in good yields. The ester derivatives of fatty acids with agarose having different molar ratios



Formation of ester derivatives in presence of DCC and DMAP

Scheme 1

(1:0.5, 1:1, 1:2) were obtained in 85–90% yield (*w/w*) yields respectively. The respective degrees of substitution (DS) were 0.25, 0.42, and 0.65 for Ag-SA and 0.27, 0.40 & 0.68 for Ag-PA (Table 1). At all levels of DS, the agarose esters (Ag-SA and Ag-PA) became insoluble in water but they were soluble in DMSO, DMF and THF at the room temperature, apparently due to the relatively greater degree of hydrophobization of the agarose polymer caused by the long chain of alkyl group. The molecular weights of Ag-SA and Ag-PA could not be measured on columns (Ultra hydragel 120, Ultra hydragel 500) due to their insolubility in water. Therefore, the molecular weights of Ag-SA and Ag-PA products were measured on styragel columns (HR 0.5 DMF, HR 4E DMF and HR 5 DMF) and the molecular weight calibration curve based on eight polystyrene standards was used. Further, a commercial agarose sample of known molecular weight was analyzed using the same method, for validation purpose. The weight average molar mass (M_w), number average molar mass (M_n) and polydispersity indices (PDI) of agarose, Ag-SA and Ag-PA are given in Table 1. The M_w and PDI data of Ag-SA and Ag-PA indicate that the agarose biopolymer backbone remained largely intact during the esterification reaction by microwave irradiation.

Characterization of Ag-SA and Ag-PA

Formation of ester bond as a result of the reaction between hydroxyl group of agarose and carboxyl termini of stearic and palmitic acids were confirmed by the appearance of the bands at 1738 and 1733 cm^{-1} respectively in their FT-IR spectra (Fig. 1). Two bands at 2852 and 1402 cm^{-1} in the spectrum of Ag-SA and 2857 and 1402 cm^{-1} represent the respective $\text{-CH}_2\text{-}$ stretching and bending vibrations of the stearic and palmitic acid chains. The intensity of the band characteristic for hydroxyl groups at $\sim 3390 \text{ cm}^{-1}$ in Ag-SA and Ag-PA derivatives is lower in comparison to that of parent agarose (3434 cm^{-1}), indicating

the formation of ester between the hydroxyl group of agarose and carboxyl group of stearic and palmitic acids. The characteristic absorption bands of agarose are seen at 1648 cm^{-1} (H-O-H, stretching vibration of bound water), 1120 cm^{-1} (C-O-C, bending vibration of glycosidic linkage) & 931 cm^{-1} (3,6-anhydro galactose) indicating that the backbone of agarose remained largely intact during the esterification reaction²⁷ (Fig. 1).

The ^{13}C NMR spectra of agarose, stearic acid, Ag-SA, palmitic acid and Ag-PA are shown in Fig. 2. The ^{13}C -NMR spectra of Ag-SA and Ag-PA exhibit peaks at 172.6 ppm and 172.9 ppm, confirming the presence of ester carbonyl group, which in stearic acid and palmitic acid appear at 180.6 ppm and 180.4 ppm respectively. The anomeric carbons of Ag-SA appear at 101.4 ppm and 97.1 ppm, of Ag-PA at 101.4 ppm and 97.4 ppm respectively as opposed 103.1 and 98.9 ppm in agarose, indicating insertion of stearic acid and palmitic acid respectively on the agarose polymer backbone. Further, the carbon resonance of the C-6 of agarose at 62.1 ppm exhibits an upfield shift to 60.1 ppm in Ag-SA and to 60.0 ppm in Ag-PA, which indicates esterification involving the C-6 hydroxyl group of agarose. Similar observation of modification at C-6 position of agarose has been reported in the literature.²³ The peaks due to the methylene carbons appear in the range 13.9–33.4 ppm in Ag-SA and 14.1–33.3 ppm in Ag-PA as opposed the slightly downfield resonances (14.5–34.2 ppm) of the methylene carbons in stearic and palmitic acids respectively. The resonances for the methylene and methine carbons of Ag-SA and Ag-PA in the range 80.1–62.9 ppm present a different pattern than that of agarose appearing in the range 82.9–62.1 ppm, corroborating again the formation of new ester derivatives. The carbon resonances were assigned by comparison with the values reported in the literature as well as with the data obtained from ChemBioDraw Ultra 11.0.²⁷

Table 1—Yield and physicochemical properties of agarose and agarose ester derivatives^a

Samples	Yield (%)	Degree of esterification (DS)	Mol. wt. (kDa)		Polydispersity index (PDI)	Soluble in
			M_w	M_n		
Agarose	NA	NA	127.571	45.690	2.792	Water
Ag-SA(1:0.5)	90	0.25	123.511	46.215	2.672	DMF, DMSO
Ag-SA (1:1)	86	0.42	121.589	45.956	2.691	DMF, DMSO
Ag-SA (1:2)	85	0.65	116.189	48.125	2.414	DMF, DMSO
Ag-PA(1:0.5)	92	0.27	124.328	45.267	2.746	DMF, DMSO
Ag-PA (1:1)	87	0.40	120.359	46.951	2.563	DMF, DMSO
Ag- PA (1:2)	85	0.68	118.189	49.923	2.367	DMF, DMSO

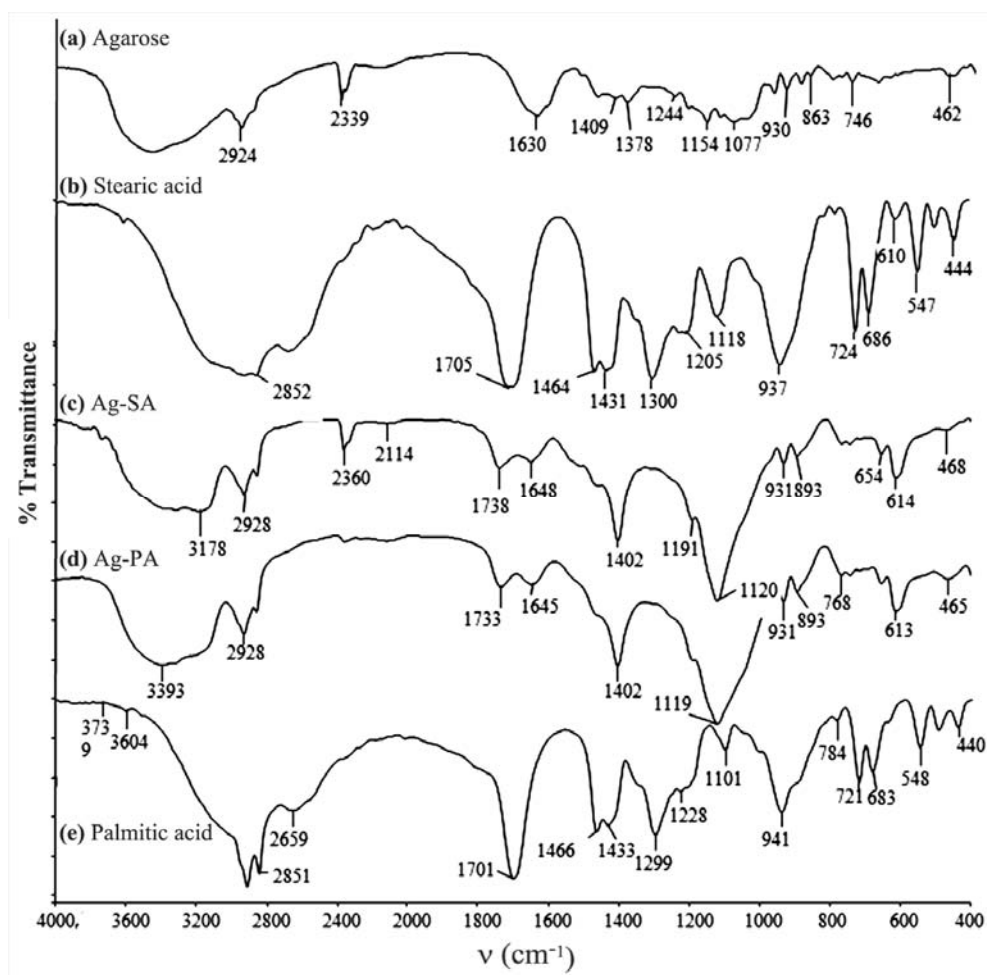


Fig. 1—FT-IR spectra of (a) agarose (b) stearic acid, (c) Ag-SA, (d) Ag-PA, and, (e) palmitic acid.

The $^1\text{H-NMR}$ spectra of Ag-SA and Ag-PA are shown in Fig. 3, and those of agarose, stearic acid, palmitic acid are depicted in the Supplementary Data (Fig. S1a-c). The $^1\text{H-NMR}$ spectrum of Ag-SA exhibits two sets of peaks of anomeric protons at 5.25–5.06 ppm and 4.88–4.69 ppm, similar to those exhibited by Ag-PA at 5.26–5.13 ppm and 4.91–4.72 ppm, indicating a pervasive anisotropy prevailing in the molecular structures of Ag-SA and Ag-PA respectively, as against the two anomeric proton resonances of agarose appearing at 5.12 ppm and 4.91 ppm (Supplementary Data, Fig. S1a). The $^1\text{H-NMR}$ spectra of the esterified agarose derivatives (Ag-SA and Ag-PA) show three protons of the terminal methyl groups of the alkyl chain, around 0.84 ppm. In Ag-SA, the proton resonances appearing in the range 2.29–2.08 ppm are attributed to the non-equivalent methylene protons alpha- to the carbonyl group, and the peaks appearing in the region 1.52–1.03 ppm to

the methylene groups of the fatty acid residue beyond the alpha-carbon. The respective proton resonances in Ag-PA are similar to those of Ag-SA. The remaining signals in the range 4.49–2.72 ppm and 4.50–2.72 ppm are attributed to the methylene and methine protons of agarose residue in Ag-SA and Ag-PA respectively, while those of agarose appear in the range 4.55–3.58 ppm.^{11,35} These data confirm the formation of Ag-SA and Ag-PA in the reaction.

The DSC thermograms in the range $-25\text{ }^\circ\text{C}$ - $25\text{ }^\circ\text{C}$ (@ $2\text{ }^\circ\text{C}/\text{min}$), of the parent agarose, Ag-SA and Ag-PA products, show T_g values (agarose: $-1.7\text{ }^\circ\text{C}$, Ag-SA: $2.2\text{ }^\circ\text{C}$ & Ag-PA: $2.8\text{ }^\circ\text{C}$), exhibiting their phase transitions (Supplementary Data, Fig. S2). The DSC thermograms in the range $30\text{--}500\text{ }^\circ\text{C}$ (@ $10\text{ }^\circ\text{C}/\text{min}$) of the parent agarose, Ag-SA and Ag-PA products show endothermic peaks at $120\text{ }^\circ\text{C}$, $110\text{ }^\circ\text{C}$ and $117\text{ }^\circ\text{C}$ for agarose, Ag-SA and Ag-PA respectively presumably because of their hydrophobicity which lowers their

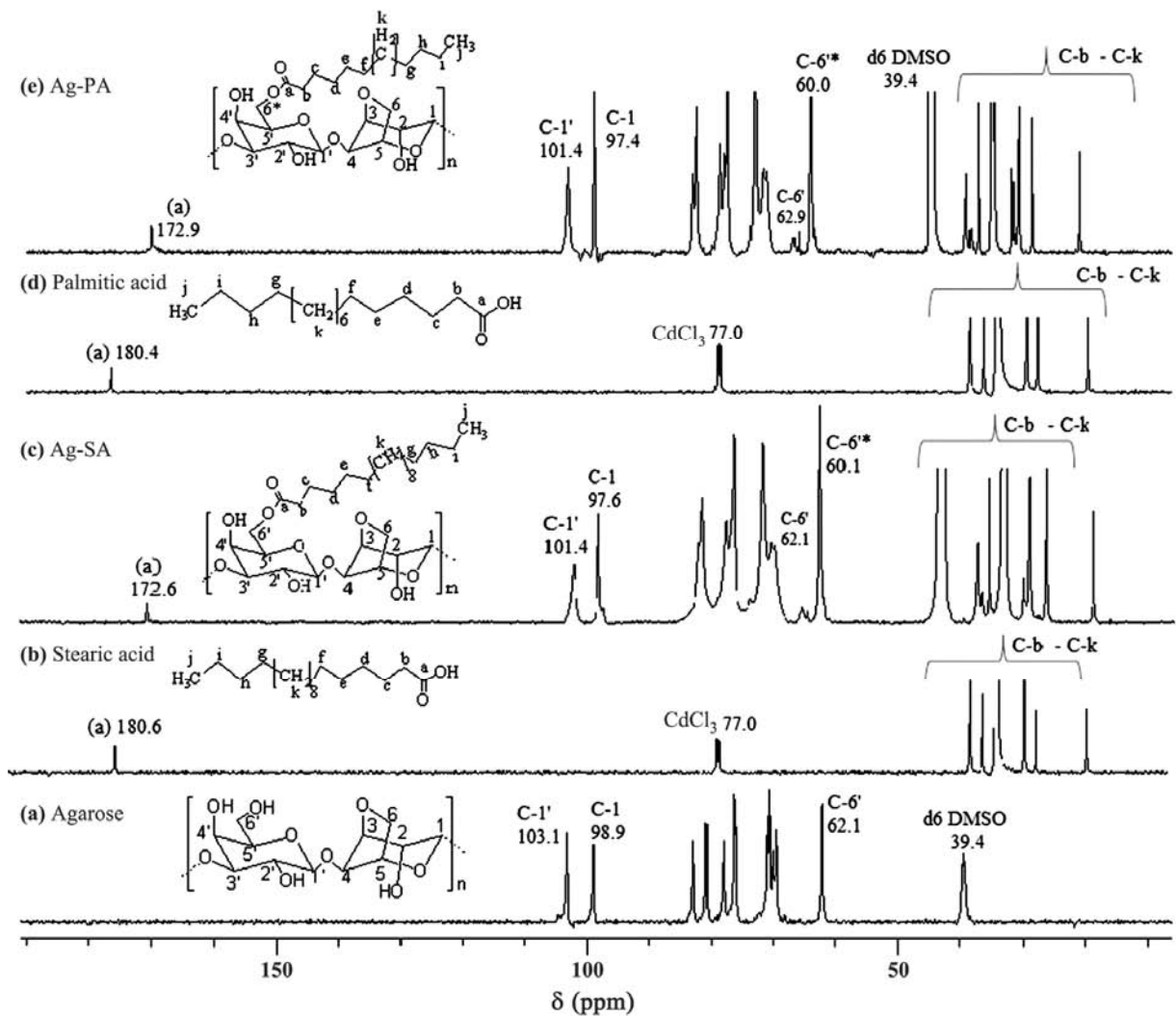


Fig. 2— ^{13}C -NMR spectra of (a) agarose (b) stearic acid (c) Ag-SA, (d) palmitic acid, and, (e) Ag-PA.

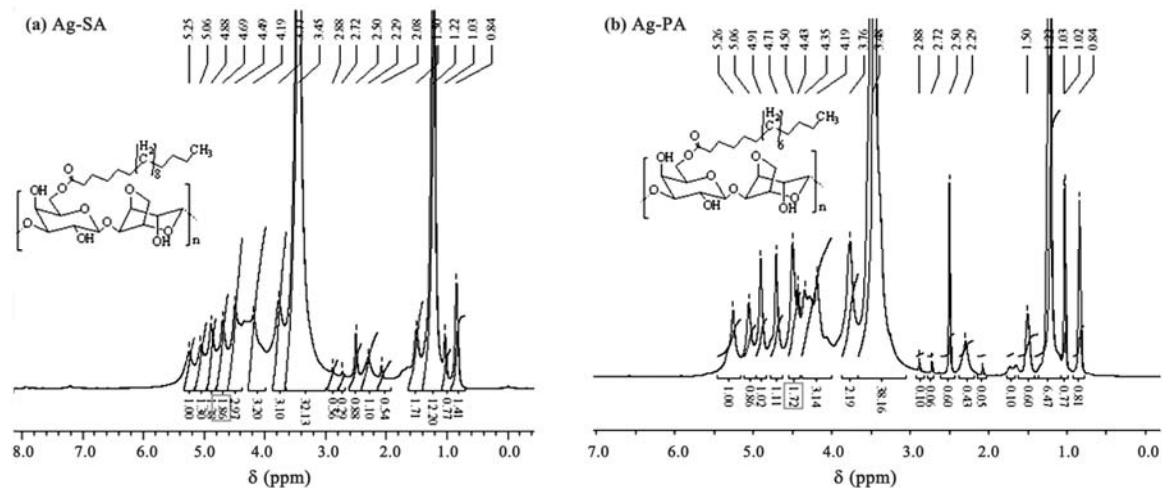


Fig. 3— ^1H -NMR spectra of (a) Ag-SA, and, (b) Ag-PA in $\text{DMSO}-d_6$ at ambient temperature.

affinity towards water molecules.^{12,36} The thermal data indicate the formation of a new products, Ag-PA and Ag-SA, which may be more amenable to processing than the parent agarose.

Self-assembled nanosized particles

To study the self-assembly of Ag-SA and Ag-PA in water, the self-aggregated nanosized particles were produced by a simple dialysis method. Agarose modified with stearic and palmitic acid formed stable nanoparticles. These nanosized particles were studied employing DLS, SEM and TEM. Self-assembled structures of Ag-SA and Ag-PA in aqueous medium were examined at a concentration 0.5%. The particle size and distribution of self-aggregates of Ag-SA and Ag-PA products in distilled water were determined by dynamic light scattering. The hydrodynamic radii, (R_h), of aggregated structures measured from DLS are shown in Fig. 4. DLS results show the formation of

micelles in the aqueous solutions of Ag-SA and Ag-PA with $R_h = 4.3$ and 4.6 nm respectively, and aggregates of vesicles of $R_h = 236.2$ and 237.1 nm respectively. The DLS showed two peaks, the first had a range of 4–10 nm which was related to polymeric micelles, and the second related to larger aggregates was between 220–250 nm.¹¹ The mean diameter of each nanoparticle was reproducible with repeated experiments and did not change with respect to its concentration. SEM images exhibited significant morphological differences between the modified agarose products and the parent agarose (Fig. 5). The SEM image of the parent agarose, which showed a cloud-like morphology that is completely transformed to particulate structures with discrete voids in Ag-SA. On the other hand, the morphology of Ag-PA appeared to have a more integrated nodular structure (Fig. 5) in *ca.* 200 nm scale. Therefore, the morphology of Ag-SA and Ag-PA

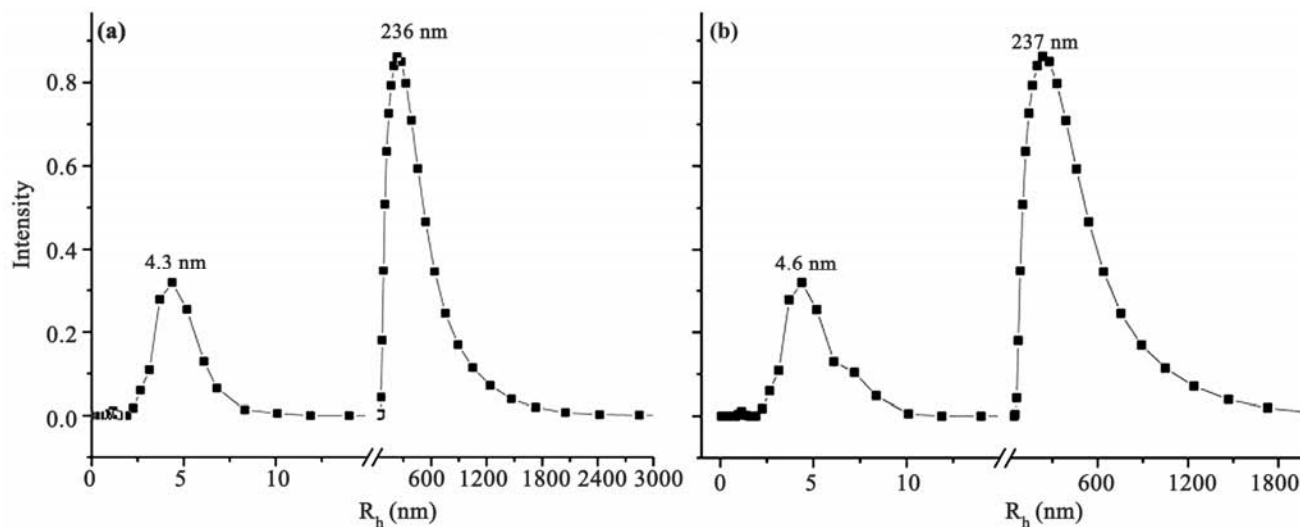


Fig. 4—The particle size distribution of (a) Ag-SA, and, (b) Ag-PA.

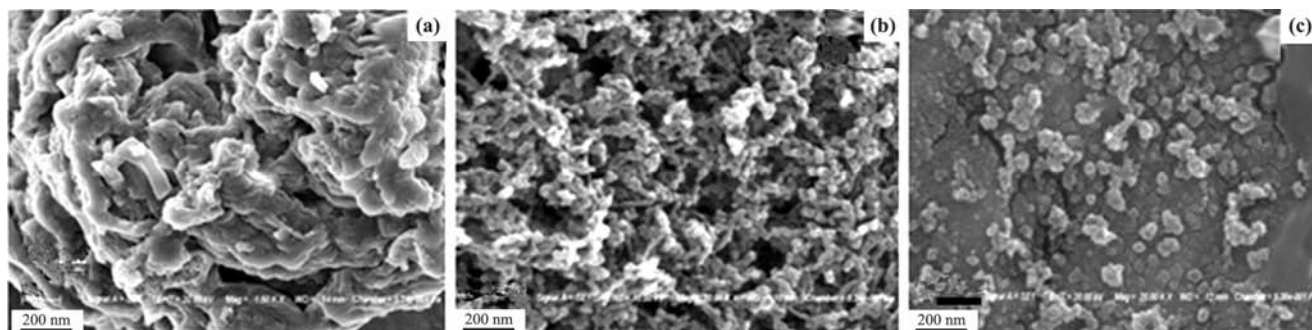


Fig. 5—SEM image of (a) agarose, (b) Ag-SA, and, (c) Ag-PA.

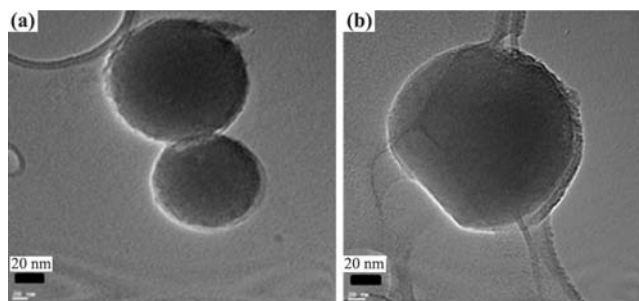


Fig. 6—TEM image of (a) Ag-SA, and, (b) Ag-PA.

nanoparticles were investigated by TEM (Fig. 6), which exhibited the presence of nanosized particles in Ag-SA and Ag-PA samples. The modified agarose polymeric nanosized particles were nearly spherical in shape, indicating their structural integrity. The mean diameter and size distribution of self-aggregates appeared to be marginally different from the results obtained by DLS measurements. For example, the size measured by the TEM methods was smaller than that obtained by the DLS method, apparently due to the difference in conditions for sample preparation and measurements.³⁵

Conclusions

Synthesis of new esters of agarose-fatty acids using stearic and palmitic acids were carried out. These hydrophobically modified agarose ester derivatives could self-assemble to form nanosized micelles and vesicles, which is being reported for the first time. The new nanosized particles of hydrophobically modified agarose may be of potential utility in the domain of drug delivery formulations.

Supplementary Data

Supplementary data associated with this article, viz., Figs S1-S2, are available in the electronic form at [http://www.niscair.res.in/jinfo/ijca/IJCA_53A\(06\)679-687_SupplData.pdf](http://www.niscair.res.in/jinfo/ijca/IJCA_53A(06)679-687_SupplData.pdf).

Acknowledgement

AKS gratefully acknowledges Council of Scientific & Industrial Research (CSIR), New Delhi, India, for the award of Emeritus Scientists' Scheme. SK and DRC are thankful to the Department of Science and Technology, New Delhi, India, for fellowships. Thanks are also accorded to CSIR for generous funding support towards infrastructure and core competency development under Analytical Discipline and Centralized Instrument Facility.

References

- Lemarchand C, Gref R & Couvreur P, *Eur J Pharm Biopharm*, 58 (2004) 327.
- Liu Z, Jiao Y, Wang Y, Zhou C & Zhang Z, *Adv Drug Del Rev*, 60 (2008) 1650.
- Chen X G, Lee C M & Park H J, *J Agric Food Chem*, 51 (2003) 3135.
- Rouzes C, Durand A, Leonard M & Dellacherie E J, *Colloids Interface Sci*, 253 (2002) 217.
- Sihorkar V & Vyas S P, *J Pharm Pharm Sci*, 4 (2001) 138.
- Rodrigues J S, Santos-Maqualhaes N S, Coelho L C, Couvreur P, Ponchel G & Gref R, *J Contr Rel*, 92 (2003) 103.
- Rouzes C, Leonard M, Durand A & Dellacherie E, *Colloids Surf B*, 32 (2003) 125.
- Shah S M, Pathak P O, Jain A S, Barhate C R & Nagarsenker M S, *Carbohydr Res*, 367 (2013) 41.
- Hassan N H, Farzaneh F F & Abolfazl H A, *Nanoparticles Based on Modified Polysaccharides*, in *The Delivery of Nanoparticles*, edited by A A Hashim, (InTech, Croatia), 2012. www.intechopen.com.
- Hu F Q, Ren G F, Yuan H, Du Y Z & Zeng S, *Colloids Surf B*, 50 (2006) 97.
- Besheer A, Hause G, Kressler J & Mader K, *Biomacromolecules*, 8 (2007) 359.
- Simi C K & Emilia Abraham T, *Bioprocess Biosyst Eng*, 30 (2007) 173.
- Li Y L, Zhu L, Liu Z, Cheng R, Meng F, Cui J H, Ji S J & Zhong Z, *Angew Chem Int Ed Engl*, 48 (2009) 9914.
- Onyukel H, Krishnadas A & Rubinstein I, *Pharm Res*, 20 (2003) 297.
- Aumelas A, Serrero A, Durand A, Dellacherie E & Leonard M, *Colloids Surf B*, 59 (2007) 74.
- Ragauskas A J, Zhang J G, Elder T J & Pu Y Q, *Carbohydr Polym*, 69 (2007) 607.
- Kwon G S, *Crit Rev Therap Drug Carrier Systems*, 20 (5) (2003) 357.
- Namazi H & Dadkhah A, *Carbohydr Polym*, 79 (2010) 731.
- Namazi H & Mosadegh M, *Recent Developments in Bio-nanocomposites for Biomedical Applications*, Chap. 18, Tiwari, A, 2011, (NOVA Science Publishers Inc, New York) 2011.
- Wang N & Wu X S, *Pharm Dev Technol*, 2 (1997) 135.
- Datta K K R, Srinivasan B, Balaram H & Eswaramoorthy M, *J Chem Sci*, 120 (2008) 579.
- Kattumuri V, Chandrasekhar M, Guha S, Raghuraman K, Katti K V K, Ghosh K & Patel R J, *Appl Phys Lett*, 88 (2006) 153.
- Zhang L M, Huang J Y, Zhang L H, Chu B & Tang S Q, *Scanning*, 32 (2010) 361.
- Araki C, *Proc Int Seaweed Symp*, 5 (1966) 3.
- Biswas A, Sharma B K, Willet J L, Vermillion K, Erhan S Z & Cheng H N, *Green Chem*, 9 (2007) 85.
- Biswas A, Shogren R L, Selling G, Salch J, Willett J L & Buchanan C M, *Carbohydr Polym*, 74 (2008) 137.
- Kondaveeti S, Prasad K & Siddhanta A K, *Carbohydr Polym*, 97 (2013) 165.

- 28 Mehta G K, Kondaveeti S & Siddhanta A K, *Polym Chem*, 2 (2011) 2334.
- 29 Kapus'niak J, Ciesielski W, Kozioł J J & Tomasik, *Eur Food Res Technol*, 209 (1999) 325.
- 30 Heinze T, Liebert T & Koschella A, *Esterification of Polysaccharides*, (Springer, Germany) 2006, www.springer.com.
- 31 Kalaskar D M, Ulijn R V, Gough J E, Alexander M R, Scurr D J, Sampson W W & Eichhorn S J, *Cellulose*, 17 (2010) 747.
- 32 Meena R, Siddhanta A K, Prasad K, Ramavat B K, Eswaran K, Thiruppathi S, Ganesan M, Mantri V A & Subbarao P V, *Carbohydr Polym*, 69 (2007) 179.
- 33 Rees D A, *Adv Carbohydr Chem Biochem*, 24 (1969) 267.
- 34 Namazi H, Fathi F & Dadkhaha A, *Sci Iranica C*, 18 (2011) 439.
- 35 Liu C G, Desai K G H, Chen X G & Park H J, *J Agric Food Chem*, 53 (2005) 437.
- 36 Fang J M, Fowler PA, Sayers C & Williams P A, *Carbohydr Polym*, 55 (2004) 283.